

Dynamic Droop Control in Microgrid for Stability Enhancement Considering RES Variation

Awan Uji Krismanto

School of Information Technology
and Electrical Engineering
University of Queensland, Australia

N. Mithulanthan

School of Information Technology
and Electrical Engineering
University of Queensland, Australia

Abraham Lomi

Electrical Engineering Department
National Institute of Technology
Malang, Indonesia

Abstract—In this paper, small signal stability analysis of a hybrid Microgrid (MG) considering RES variations is addressed. As wind speed or solar irradiance fluctuates, active power output from DGs might vary significantly. Hence, the power sharing scheme would change considerably. Dynamic droop-gain control is proposed to deal with the RES change and maintain the stability of MG. The proposed control method provides adjustable power sharing strategies to manage RES fluctuation and ensure frequency and voltage regulation of each DGs. Eigenvalues analysis and time domain simulation suggest that at high wind speed and solar irradiance the damping ratio of critical modes and dynamic performance of DG units defer significantly. As the dynamic droop controller implemented, the damping performance and stability margin of the hybrid MG were improved in different operating condition, ensuring stable MG operation in most of RES conditions.

Keywords—*Microgrid, RES variations, variable droop, power sharing, small signal stability.*

I. INTRODUCTION

One of the main concerns with single distributed power generation (DG) based on renewable energy resources (RES) is how to ensure stable and continuous electricity supply. To deal with this concern, a cluster of DG units needs to be coordinated into a supervised power system as Microgrid (MG). The beneficial features of MG concept encourage more integration of RES. It has emerged as a powerful platform in power system due to its advantages for improving power quality and providing more reliable electricity services for remote areas. Furthermore, ancillary services regarding frequency support and voltage regulation could be potentially introduced by MG [1].

Though MG facilitates seamless integration of renewable energy resources (RES), it brings novel challenges to power system operation and control [2]. From a small signal stability point of view, less inertia characteristic of DG unit in MG might deteriorate system damping and dynamic performance. The decrease in aggregated system inertia could result in more oscillatory condition when MG is subjected to small disturbance [3]. In addition, RES variations, introduce a more fluctuating condition of voltage and frequency, which eventually lead to unstable generated power within MG.

During islanding operation, MG control should be able to achieve accurate power sharing among DGs while maintain the voltage and frequency within the specified limits [4].

Power sharing and frequency regulation are realised by decentralised control scheme based on static droop control method as presented in [3, 5]. Since the fluctuated condition of RES significantly influences power sharing in MG, the existing droop control method should be modified to handle RES uncertainty. In [1, 6], regulation of active droop gain as a function of available power from wind speed and de-loaded factor in a Wind Energy Conversion System (WECS) is presented. Frequency in MG should be monitored continuously, maintain synchronization among DGs and stable MG operation. The frequency support can be approached by connecting energy storage devices to restore the frequency deviation. However, due to high cost of energy storage, each of DG unit should participate in frequency regulation without depending on external resources. To ensure sufficient power preserve for frequency regulation purpose, de-loading control method might be implemented in WECS and PV based DGs [6, 7]. Adaptive droop control method was proposed in [4] to improve the dynamic response of MG due to load change scenarios without considering RES change.

Only few research were conducted to investigate the small signal stability performance of MG considering RES variation. The focus of this paper is to develop a dynamic droop control strategy to ensure accurate power sharing and enhance the small signal stability performance of MG in islanding operation to deal with the variation of RES. Impact of wind speed and solar irradiance change on power sharing and dynamic response of Hybrid MG comprising of WECS, PV, and diesel engine (DE) are investigated. A comprehensive model of each DG units is developed to provide a complete picture of MG small signal stability performance. Dynamic droop control method is proposed to enhance MG small signal stability and regulation of MG voltage and frequency during RES fluctuation. Oscillatory condition and dynamic response of MG in different power sharing strategies will be evaluated by monitoring trajectories of critical eigenvalues and dynamic response through time domain simulations.

The remainder of the paper is organized as follows. A comprehensive system modeling of DE, WECS and PV DG units involving network and load dynamics are presented in Section II. Section III presents proposed dynamic droop gain control method. The simulation results are presented and discussed in Section IV. Eventually, conclusions and

II. MICROGRID MODEL DEVELOPMENT

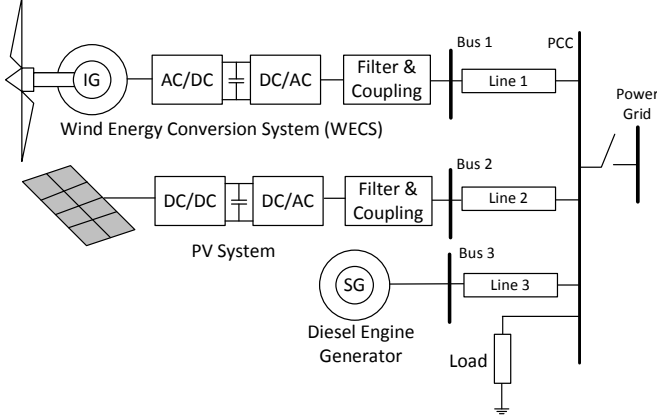


Fig. 1. Microgrid Model.

Fig.1 shows the investigated MG system that consists of three DG units and a central load. The first RES based DG unit employs fully rated WECS type with back-to-back (AC/DC/AC) inverter. PV system with a DC/DC and DC/AC inverter is selected as second DG unit. The aforementioned DGs are selected due to its beneficial features of full energy conversion and stability. The third DG unit is a Diesel Engine Generator (DE), which is connected to ensure power balance during the shortfall of RES power from WECS and PV. The synchronization procedure among DGs is derived from [3].

State space equations of lines impedance is given by

$$\Delta \dot{x}_{line} = A_{line} \Delta x_{line} + B_{line} \Delta v_{blineDQ} + B_{line_pcc} \Delta v_{pcc} + B_{linede} \Delta \omega_{ref} \quad (1)$$

Where $\Delta x_{li} = [\Delta i_{lineDQ}]^T$, $\Delta v_{blineDQ} = [\Delta v_{bDQ}]^T$, $\Delta v_{pcc} = [\Delta v_{pccDQ}]^T$. B_{line} and B_{line_pcc} represent line input and line-PCC bus connection matrices respectively. The connection between line and DE is dictated by and B_{linede} .

General load impedance model is presented by the following state equation (5).

$$\Delta \dot{x}_{lo} = A_{lo} \Delta x_{lo} + B_{lo} \Delta v_{pccDQ} + B_{lode} \Delta \omega_{ref} \quad (2)$$

Where $\Delta x_{lo} = [\Delta i_{loadDQ}]^T$. B_{lo_pcc} and B_{lode} represent connection matrices between load-PCC and load-DE respectively.

Diesel Engine (DE) Generator Model

Detailed state space model of DE generator is derived from [8, 9]. State variables of DE consist of rotor, stator, and field winding currents in the $d-q$ axis. While, input variables are presented as mechanical torque, field winding, and stator voltage. As a reference, DE provides a reference frequency signal for WECS and PV. State space equation of DE generator is stated as given in (6).

$$\Delta \dot{x}_{de} = A_{de} \Delta x_{de} + B_{de} \Delta u_{de} + B_{vde} \Delta v_{b3} \quad (3)$$

Where

$$\Delta x_{de} = [\Delta i_{sd} \quad \Delta i_{sq} \quad \Delta i_{fd} \quad \Delta i_{kd} \quad \Delta i_{kq1} \quad \Delta i_{kq2} \quad \Delta \omega_{ref} \quad \Delta \delta_{ref}]^T$$

$$\Delta u_{de} = [\Delta v_{fd} \quad \Delta T_{Mde}]^T, \Delta v_{b3} = [\Delta v_{b3dq}]^T$$

B_{de} and B_{vde} represent input and connection matrices between DE-local bus, respectively.

WECS Model

Fully rated WECS mainly consists of a wind turbine, induction generator, power electronic devices and associated controllers. AC/DC/AC converter model is obtained from integration of subsystems in [10-12]. While, induction generator model is derived from [8, 13]. WECS control is comprising of generator and grid side converter control. Regulation of DC link voltage and variable speed operation capability of induction machine are functionalized by AC/DC converter through flux oriented control (FOC) scheme [13]. Detailed model of generator side controller is derived from [14].

The control algorithm of DC/AC grid side inverter is depicted in Fig. 2. The inverter control can be divided into primary and secondary controller [3, 5]. The primary control facilitates power sharing capability while provides frequency support and voltage restoration. These control purposes is realized by proposed dynamic droop control method.

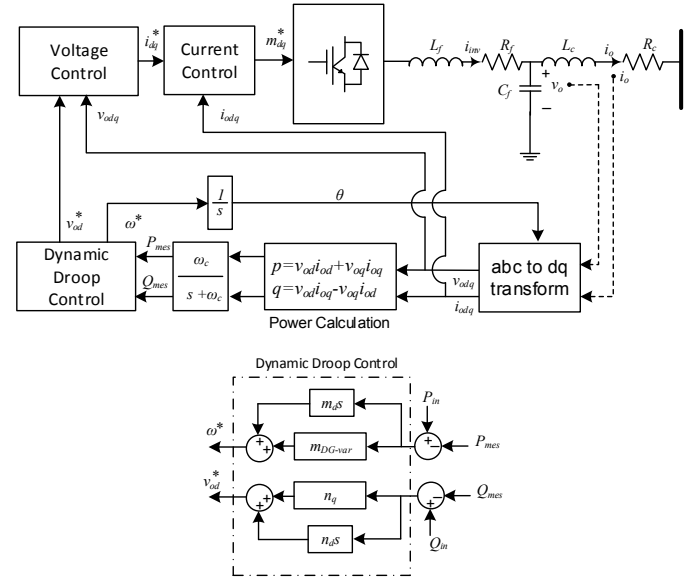


Fig. 2. Power Circuit and proposed dynamic droop control of DGs grid side inverter in Microgrid.

Average active and reactive power are dictated as

$$\Delta P_{meas} = \{\omega_c / (s + \omega_c)\} p \rightarrow \{d \Delta P_{meas} / dt\} = \omega_c p - \omega_c \Delta P_{meas} \quad (4)$$

$$\Delta Q_{meas} = \{\omega_c / (s + \omega_c)\} q \rightarrow \{d \Delta Q_{meas} / dt\} = \omega_c q - \omega_c \Delta Q_{meas} \quad (5)$$

While, frequency (ω^*) and voltage (v^*) reference values as a function of droop parameters are given by (6) and (7) respectively.

$$\omega^* = \omega_n - m_{DG-var} \Delta P_{meas} \quad (6)$$

$$v_{od}^* = v_n - n_q \Delta Q_{meas} \quad (7)$$

ω_n and v_n represent the nominal values of frequency and voltage respectively. The detailed calculation of dynamic droop (m_{DG-var}) value will be presented in section III.

The obtained reference values from primary control become input variables for secondary control comprising of voltage and current controller loop. Voltage controller is responsible for generating reference values for inner current loop which generates modulation signal for inverter (m_{dq}^*). The state equations of voltage and current controller are given by equations (8) and (9), respectively.

$$\begin{aligned} \dot{[\Delta\varphi_{dq}]} &= [0][\Delta\varphi_{dq}] + \begin{bmatrix} 1 & 0 & -1 & 0 \\ 0 & 1 & 0 & -1 \end{bmatrix} \begin{bmatrix} v_{odq}^* \\ v_{odq} \end{bmatrix} \\ \dot{[i_{dq}^*]} &= \begin{bmatrix} K_{iv} & 0 \\ 0 & K_{iv} \end{bmatrix} [\Delta\varphi_{dq}] + \begin{bmatrix} K_{pv} & 0 & -K_{pv} & -\omega C_f \\ 0 & K_{pv} & \omega C_f & -K_{pv} \end{bmatrix} \begin{bmatrix} v_{odq}^* \\ v_{odq} \end{bmatrix} \quad (8) \\ \dot{[\Delta\beta_{dq}]} &= [0][\Delta\beta_{dq}] + \begin{bmatrix} 1 & 0 & -1 & 0 \\ 0 & 1 & 0 & -1 \end{bmatrix} \begin{bmatrix} i_{odq}^* \\ i_{odq} \end{bmatrix} \\ \dot{[m_{dq}^*]} &= \begin{bmatrix} K_{ic} & 0 \\ 0 & K_{ic} \end{bmatrix} [\Delta\varphi_{dq}] + \begin{bmatrix} K_{pc} & 0 & -K_{pc} & -\omega L_f \\ 0 & K_{pc} & \omega L_f & -K_{pc} \end{bmatrix} \begin{bmatrix} i_{odq}^* \\ i_{odq} \end{bmatrix} \quad (9) \end{aligned}$$

Where φ_{dq} and β_{dq} respectively represent auxiliary state variables of voltage and controller loop.

A complete model for fully rated converter WECS is then derived by integrating state equations of induction generator model in [8, 15], AC/DC/AC inverter model in [11, 12], FOC controller at generator side and droop controller at grid side converter [3, 14]. Moreover, detailed modeling procedure of both controllers is derived from [3, 5, 13, 15]. State space equation of WECS is given by

$$\begin{aligned} \dot{\Delta x}_w &= A_w \Delta x_w + B_w \Delta u_w + B_{vw} \Delta v_{b1} + B_{wd} \Delta \omega_{ref} \\ \Delta x_w &= \begin{bmatrix} \Delta i_{sdq} & \Delta i_{rdq} & \Delta \omega_{rw} & \Delta \gamma & \Delta \rho_{wdq} & \Delta i_{dq} & \Delta v_{indq} \\ \Delta \delta_w & \Delta P_w & \Delta Q_w & \Delta \varphi_{dq} & \Delta \beta_{dq} & \Delta v_{dcout} & \Delta i_s \\ \Delta v_{dc} & \Delta i_{invdq} & \Delta v_{odq} & \Delta i_{odq} \end{bmatrix}^T \quad (10) \end{aligned}$$

In which, γ and ρ_{wdq} are the auxiliary variables for FOC controller. B_w is input matrix of WECS. Connection matrices of WECS to the line and DE as reference DG unit are given by B_{vw} and B_{wd} respectively.

PV Model

Proposed model of two stages PV unit consists of PV array, DC/DC and DC/AC inverter. Averaged model of DC/DC is derived from [16]. While, DC/AC model is adopted from [10, 11]. Regulation of DC link voltage between DC/DC and DC/AC inverter is realized by comparing DC link voltage (Δv_{dc}) to reference value (Δv_{dc_ref}). The obtained error is then regulated by PI controller to generate duty cycle (Δd_{pv}) control signal for DC/DC converter. State space equation for DC link controller ($\Delta \rho_{pv}$) is given by

$$\dot{\Delta \rho}_{pv} = [0] \Delta \rho_{pv} + [1 \ -1] \begin{bmatrix} \Delta v_{dc_ref} \\ \Delta v_{dc} \end{bmatrix}$$

$$\Delta d_{pv} = \begin{bmatrix} K_{ipv} \\ K_{ppv} \end{bmatrix} \Delta \rho_{pv} + \begin{bmatrix} K_{ppv} & -K_{ppv} \end{bmatrix} \begin{bmatrix} \Delta v_{dc_ref} \\ \Delta v_{dc} \end{bmatrix} \quad (11)$$

Similar control algorithm as in WECS was adopted to develop grid side inverter control in PV system. Detailed model of PV is obtained by combining state equation of DC/DC, DC/AC, and control system in (8), (9) and (11). State space model of PV system can be stated as given in (15).

$$\begin{aligned} \dot{\Delta x}_{pv} &= A_{pv} \Delta x_{pv} + B_{pv} \Delta u_{pv} + B_{vpv} \Delta v_{b2} + B_{pvd} \Delta \omega_{ref} \\ \Delta x_{pv} &= \begin{bmatrix} \Delta i_b & \Delta i_s & \Delta v_b & \Delta v_{dc} & \Delta \rho_{pv} & \Delta \delta_{pv} & \Delta P_{pv} \\ \Delta Q_{pv} & \varphi_{pvdq} & \Delta \beta_{dqv} & \Delta i_{invdq} & \Delta v_{odq} & \Delta i_{odq} \end{bmatrix}^T \quad (12) \end{aligned}$$

State variables for DC/DC and inverter control in PV system are presented by ρ_{pv} , φ_{dqv} and β_{dqv} . B_{pv} is input matrix of PV. Connection matrices of PV to the appropriate line and DE as reference DG unit are given by B_{vpv} and B_{pvd} respectively.

III. DYNAMIC DROOP CONTROL IN MICROGRID

The droop gain values should be adjusted continuously to ensure accurate power sharing in accordance with the fluctuating condition of wind speed and solar irradiance. Moreover, to ensure sufficient power preserve for frequency regulation purpose, the WECS and PVs were operated below its maximum operating point [6, 7]. A proposed dynamic droop parameter considering RES variation and power preserve for frequency regulation purpose is given by (13).

$$m_{DG-var} = \left(m_{max} - (m_{max} - m_{min}) \left\{ \frac{P_{input}}{P_{max}} \right\} \right) \quad (13)$$

Where P_{input} and P_{max} represent available input power from RES and maximum power capacity of DGs respectively. m_{max} and m_{min} corresponded to maximum and minimum active gain control setting respectively.

By using (13) and substitute the input power equations of WECS in [2] and PV in [17], the dynamic droop in WECS and PV based DGs are given by

$$m_{WECS-var} = m_{max} - (m_{max} - m_{min}) \left\{ \frac{0.5 \rho C_{opt} (\lambda_{opt}, \beta) A_r v_{w0}^3}{P_{max}} \right\} \quad (14)$$

$$m_{PV-var} = m_{max} - (m_{max} - m_{min}) \left\{ I_{sc} \left(\frac{G_0}{G_{ref}} \right) - I_s e^{\frac{qV_{pv}}{nkTN_s}} \right\} \quad (15)$$

Where v_{w0} and G_0 represent an initial condition of wind speed and solar irradiance around a certain operating point respectively. For WECS based DG unit, it is assumed that power input from a certain wind speed condition is a function of a given wind speed with constant tip speed ratio and blade pitch angle.

System damping and dynamic response enhancement might be realized by incorporating derivative components to (6) and (7). Combination of dynamic and derivative droop control strategies is given by

$$\omega^* = \omega_n - m_{DG-var} (\Delta P_{in} - \Delta P_{meas}) - m_{pd} \frac{d(\Delta P_{in} - \Delta P_{meas})}{dt} \quad (16)$$

$$v_{od}^* = v_n - n_q (\Delta Q_{in} - \Delta Q_{meas}) - n_{qd} \frac{d(\Delta Q_{in} - \Delta Q_{meas})}{dt} \quad (17)$$

Where ΔP_{in} represents active power generated by each of DGs corresponded to available RES power. Derivative active and reactive power droop gain are presented by m_{pd} and n_{qd} respectively. It is assumed that generated power from RES only consists of active power. Hence, the generated reactive power input (ΔQ_{in}) is assumed to be zero [18].

By substituting (4) and (5) into (16) and (17), the small signal model of the proposed droop control method is calculated by

$$\omega^* = \omega_n - m_{DG-var} (\Delta P_{in} - \Delta P_{meas}) - m_{pd} (\omega_c p - \omega_c \Delta P_{meas}) \quad (18)$$

$$v_{od}^* = v_n - n_q \Delta Q_{meas} - n_{qd} (\omega_c q - \omega_c \Delta Q_{meas}) \quad (19)$$

Active and reactive droop gains selection are conducted as a compromise among accurate power sharing, enhancement of dynamic response and voltage regulation. However, since MG small signal stability less sensitive to reactive droop gain variation as reported in [3, 4, 19], the proposed study is focused on active power sharing and small signal stability performance of MG under RES variation. Hence, reactive power droop gains in each DGs are maintained constant throughout this work.

IV. RESULTS AND DISCUSSIONS

A complete model of PV, WECS, and DE was developed by adopting parameters of WECS and DE from [8, 14, 15]. The small signal model of 3 MVA WECS, PV and DE based DGs were combined with state space model of the network to supply 5 MW load. The DE was connected to the MG to overcome the shortfall power from PV and WECS due to RES variations. It is assumed that the eigenvalues corresponded to DE was asymptotically stable. Hence, modal analysis was focused on critical eigenvalues associated with active power output from WECS and PV. Dynamic performance of the MG with variation of wind speed and solar irradiance is investigated through eigen-trajectories and time domain simulation.

Small signal stability performance of MG with static droop and proposed dynamic droop control were evaluated. In static droop control scheme, the active power droop gain of WECS and PV were set at 8%. While for dynamic droop control strategy, the active power droop gain was adjusted according to the variation of wind speed and solar irradiance by using equation (14) and (15) respectively. In this paper, a maximum and minimum active power droop setting were set at 8% and 4% respectively. Hence the dynamic droop gain might be varied within the specified limit. Furthermore, to improve system response, the derivative gain control in dynamic droop method is tuned at 0.00001.

Fig.3 shows the trajectories of sensitive modes corresponded to the active power output of WECS ($\lambda_{42,43}$) and PV ($\lambda_{45,46}$) when wind speed varied from 5 m/s to 20 m/s and

solar irradiance was assumed constant at 1000 W/m². It was clearly seen that in the static control scheme, sensitive modes from WECS deviated significantly during the variation. As wind speed increased, MG dynamic response and damping performance deteriorated remarkably. Even, the sensitive modes were unstable when the wind speed exceed 15 m/s. It was also monitored that implementing proposed dynamic droop control result in significant enhancement of oscillatory condition. Indicated by significant left shift trajectories of modes $\lambda_{42,43}$. While modes $\lambda_{45,46}$ relatively stable in its position both in investigated control strategies.

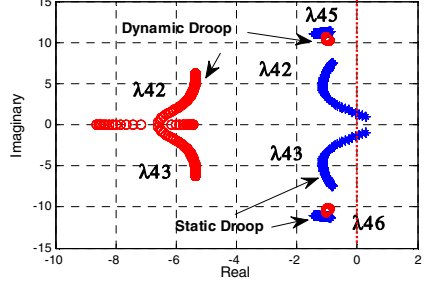


Fig. 3. Sensitive Modes of DGs due to the variation of wind speed.

Table 1 represents damping ratio of the investigated modes during variation of wind speed for both droop control strategies, under investigation. In static droop control scheme, MG was stable and the oscillation was well damped when the wind speed fluctuated from 7m/s to 11 m/s, indicated by variation of damping ratio of modes $\lambda_{42,43}$ from 7.6% to 14.1%. The critical situation occurred at 14 m/s wind speed, indicated by 3% damping ratio on modes $\lambda_{42,43}$. Moreover, the MG become unstable when the wind speed exceed 15m/s. The damping ratio of modes of $\lambda_{45,46}$ deteriorated moderately from 14.8% to 9%. However, it could be considered stable as the damping ratio of the modes was more than 5%.

Table 1. Damping Ratio of the sensitive modes in various wind speed

Modes	Control Scheme	Damping Ratio (ζ) in Various Wind Speed				
		7 m/s	9 m/s	11m/s	14m/s	15m/s
$\lambda_{42,43}$	Static	7.6%	10.1%	14.1%	3%	-4.5%
	Dynamic	66.8%	71.5%	81.2%	89.5%	98.5%
$\lambda_{45,46}$	Static	14.8%	13.5%	12%	9.8%	9%
	Dynamic	9.1%	9.5%	9.9%	10.2%	10.1%

The system dynamic response significantly improved when dynamic droop control implemented. It was clearly seen that the oscillatory condition related to the modes of $\lambda_{42,43}$ was well damped in all wind speed condition. The damping ratio was significantly improved in the range of 66.8% to 98.5%, ensuring stable condition of MG and smooth transition of power sharing due to wind speed change. It was observed that the damping ratio of modes of $\lambda_{45,46}$ was slightly deteriorated when dynamic droop control was applied. However, it was monitored that the corresponded modes relatively stable in its position when system was subjected to wind speed variation. Only small enhancement of the damping ratio from 9.1% to 10.2% was monitored.

Fig. 4 represents trajectories of sensitive modes when solar irradiance varied from 800 W/m^2 to 1100 W/m^2 . The terminal voltage of PV array is not influenced significantly as the solar irradiance fluctuated. Furthermore, since ambient temperature was also assumed constant, a variation in solar irradiance would not affect the system dynamic response as significant as a variation on wind speed. Hence, it was noticeable that both of the observed modes were less sensitive to fluctuation of solar irradiance. Indicated by a small movement of modes in static droop gain control technique. Improvement of stability performance was observed as sensitive eigenvalues corresponded to WECS active power moved to the left-hand side when dynamic control was applied. The eigenvalues analysis suggested that WECS based DGs was more sensitive to small disturbance or change in RES than two stages PV system based DGs.

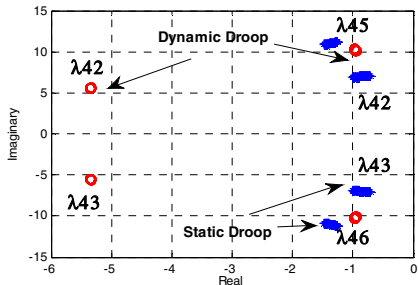


Fig. 4. Sensitive Modes of DGs due to the variation of solar irradiation.

Damping ratio of the sensitive modes when the MG was subjected to solar irradiance variation is presented in Table.2. The dynamic response of sensitive modes of $\lambda_{42,43}$ significantly improved from 10% to 12% with static droop to around 69% with dynamic droop strategy. Eventhough, the damping condition of modes of $\lambda_{45,46}$ decreased moderately from around 12% to 9.4% when the dynamic droop scheme applied, the corresponded modes relatively stable in its position during solar irradiance variation since the damping ratio was higher than critical value of 5%.

Table 2. Damping Ratio of the sensitive modes in various solar irradiance

Modes	Control Scheme	Damping Ratio (ζ) in various Solar Irradiance			
		700 (W/m ²)	800 (W/m ²)	900 (W/m ²)	1000 (W/m ²)
$\lambda_{42,43}$	Static	10.9%	11.3%	11.6%	12%
	Dynamic	69%	69%	69.1%	69.1%
$\lambda_{45,46}$	Static	13%	12.7%	12.6%	12.3%
	Dynamic	10.9%	9.4%	9.4%	9.4%

Stability margin enhancement corresponded to the system operating domain was also identified. Using dynamic control strategy, the investigated hybrid MG can be operated in all of the wind speed and solar irradiance condition. While, in static droop scheme, the operation range of MG should be limited below 15 m/s wind speed to ensure stable MG operation.

Verification of proposed control system to handle RES variation in MG system was conducted using time domain simulation in MATLAB Simulink. A step change of RES regarding wind speed and solar irradiance changes were

considered to excite the monitored modes. Furthermore, comparison of MG dynamic response with static and proposed dynamic control during RES changes was evaluated.

Dynamic response of each DGs during wind speed fluctuation both in static and dynamic droop control strategies is depicted in Fig.5. The first scenario considered small wind speed variation from 8m/s to 10 m/s and eventually to 7 m/s. While, solar irradiance was assumed constant at 1000 W/m^2 . Enhancement of MG small signal stability was observed as dynamic droop control scheme was implemented. Indicated by more damped of the oscillatory condition during RES change. It was also monitored that the proposed control algorithm was able to follow the change in wind speed by changing the adaptive droop gain autonomously hence the generated power from DGs matched with demanded 5 MW load demand.

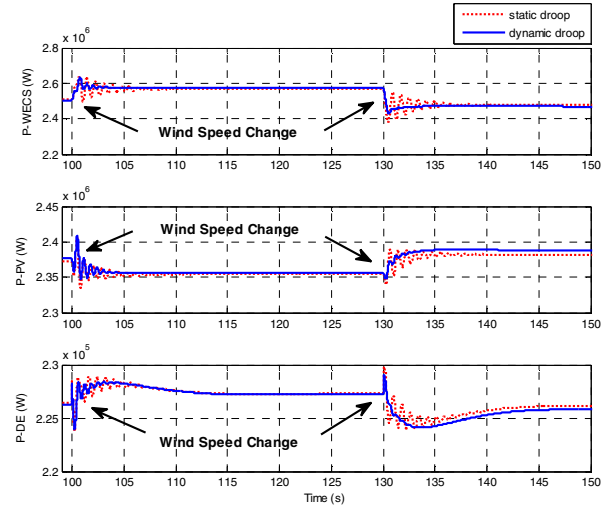


Fig. 5. Power Sharing during wind speed change.

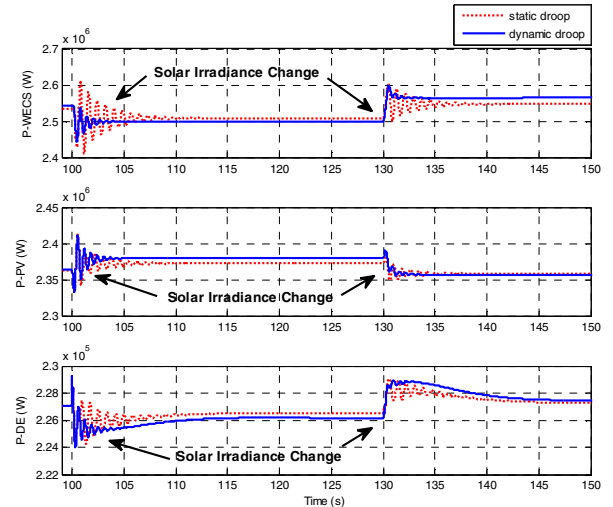


Fig. 6. Power Sharing during solar irradiance change

As presented in Fig.6, the performance of the proposed dynamic droop control was also evaluated under the second scenario with a variation of solar irradiance. To realize those study case, it was considered that solar irradiance fluctuated

from 800 W/m^2 to 1000 W/m^2 and 700 W/m^2 while the wind speed was assumed constant at 10 m/s . Enhancement of MG small signal stability was monitored. The oscillatory amplitude significantly reduced, and the stable steady state condition was achieved faster compared with static droop control scheme. The monitored time domain simulations were consistent to the previous eigenvalues analysis. The system damping significantly improved and more seamless dynamic response during RES change were observed as dynamic droop control applied.

The dynamic droop control method not only ensures the MG stability but also enhances frequency and voltage regulation. Fig.7 represented system frequency and bus voltage when a small variation on RES occurred. In static droop control, WECS and PV did not participate in frequency and voltage regulation hence more oscillatory condition and higher overshoot amplitude were experienced. On the other hand, the proposed dynamic control method was feasible to provide an additional contribution from DG unit to support system frequency and maintain voltage stability during the occurrence of RES variation. The improvements were indicated by lower undershoot and less deviation of system frequency.

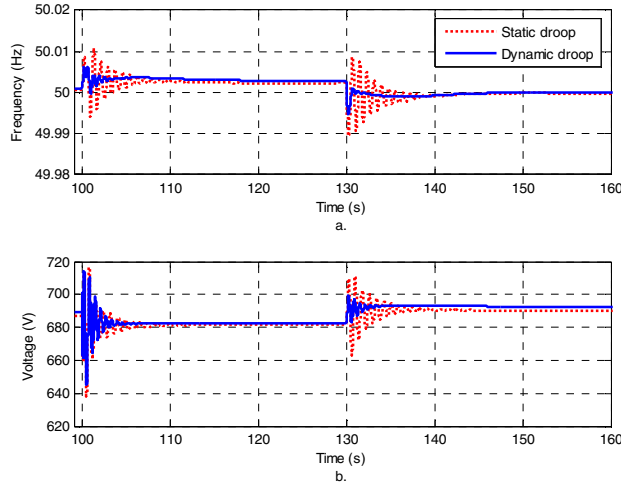


Fig. 7. System frequency and bus (a) voltage (b) during RES change.

V. CONCLUSIONS

In this paper, a small signal stability analysis of hybrid MG system considering wind speed and solar irradiance variations was presented. As RES varied, power sharing scheme among DG unit in MG changed considerably. Eigenvalues analysis and time domain simulation suggested that at high wind speed, the small signal stability performance of MG deteriorated differently. A more oscillatory condition in MG was monitored when wind speed fluctuated. While, the only small effect on dynamic performance was experienced when solar irradiance varied. To deal with the RES change, dynamic droop control method was proposed. It was monitored that the proposed droop control method preserves dynamic response

and stability performance of each DG units at different power sharing scheme correlated to fluctuating RES conditions.

REFERENCES

- [1] M. F. M. Arani and Y. A.-R. I. Mohamed, "Analysis and Impacts of Implementing Droop Control in DFIG-Based Wind Turbines on Microgrid/Weak-Grid Stability," *IEEE Transaction on Power System*, vol. 30, pp. 385-396, 2015.
- [2] M. Shahabi, M.R.Haghifam, M.Mohamadian, and S. A. Nabavi-Niaki, "Microgrid Dynamic Performance Improvement Using a Doubly Fed Induction Wind Generator," *IEEE Transaction on Energy Conversion*, vol. 24, pp. 137-145, 2009.
- [3] N. Pogaku, M. Prodanovic, and T. C. Green, "Modeling, analysis and testing of autonomous operation of an inverter-based microgrid," *IEEE Transactions on Power Electronics*, vol. 22, pp. 613-625, Mar 2007.
- [4] Y. A.-R. I. Mohamed and E. F. El-Saadany, "Adaptive Decentralized Droop Controller to Preserve Power Sharing Stability of Paralleled Inverters in Distributed GenerationMicrogrids," *IEEE Transaction on Power Electronics*, vol. 23, pp. 2806-2816, 2008.
- [5] A. Kahrobaeian and Yasser Abdel-Rady I.Mohamed, "Analysis and Mitigation of Low-Frequency Instabilities in Autonomous Medium-Voltage Converter-Based MicrogridsWith Dynamic Loads," *IEEE Transaction on Industrial Electronics*, vol. 61, pp. 1643-1658, 2014.
- [6] K. V. Vidyanandan and N. Senroy, "Primary Frequency Regulation by Deloaded Wind Turbines Using Variable Droop," *IEEE Transaction on Power System*, vol. 28, pp. 837-846, 2013.
- [7] P. P. Zarina, S. Mishra, and P. C. Sekhar, "Exploring frequency control capability of a PV system in a hybrid PV-rotating machine-without storage system," *Electrical Power and Energy Systems*, vol. 60, pp. 258-267, 2014.
- [8] P. C. Krause, O. Waszczuk, and S. D. Sudhoff, *Analysis of Electric Machinery and Drive System 2nd Edition*: Wiley-Interscience, 2002.
- [9] C. E. Ugalde-Loo and J. B. Ekanayake, "State-Space Modelling of Variable-Speed Wind Turbines: A Systematic Approach," presented at the Sustainable Energy Technologies (ICSET), Kandy, Sri Lanka, 2010.
- [10] R. Wu, S. B. Dewan, and G. R. Slemon, "A Pwm Ac-to-Dc Converter with Fixed Switching Frequency," *IEEE Transactions on Industry Applications*, vol. 26, pp. 880-885, Sep-Oct 1990.
- [11] R. Wu, S. B. Dewan, and G. R. Slemon, "Analysis of an AC-to-DC Voltage Source Converter using PWM with Phase and Amplitude Control," *IEEE Transactions on Industry Application*, vol. 27, p. 12, 1991.
- [12] N. A. Rahim and J. E. Quiccoe, "Small Signal Model and Analysis of A Multilevel Feedback Control Scheme for Three Phase Voltage Source UPS Inverter," in *Proceedings of Power Electronics Specialist Conference*, Bovenlo, Italy, 1996, pp. 188-194.
- [13] O. Anaya-Lara, N. Jenkins, J. Ekanayake, P. Cartwright, and M. Hughes, *Wind Generation: Modelling and Control*: John Wiley & Sons, Ltd, 2009.
- [14] BinWu, Y. Lang, N. Zargari, and S. Kouro, *Power Conversion and Control of Wind Energy Systems*: Wiley, 2011.
- [15] C. E. Ugalde-Loo, J. B. Ekanayake, and N. Jenkins, "State-Space Modeling of Wind Turbine Generators for Power System Studies," *IEEE Transaction on Industry Application*, vol. 48, pp. 223-232, 2013.
- [16] R. W. Erickson and D. Maksimovic, *Fundamental of Power Electronics Second Edition*. University of Colorado Boulder, Colorado: Kluwer Academic Publisher, 2001.
- [17] Y. T. Tan, D. S. Kirschen, and N. Jenkins, "A Model of PV Generation Suitable for Stability Analysis," *IEEE Transaction on Energy Conversion*, vol. 19, pp. 748-755, 2004.
- [18] J. Kim, J. M. Guerrero, P. Rodriguez, R. Teodorescu, and K. Nam, "Mode Adaptive Droop ControlWith Virtual Output Impedances for an Inverter-Based Flexible AC Microgrid," *IEEE Transaction on Power Electronics*, vol. 26, pp. 689-701, 2011.
- [19] E. Barklund, N. Pogaku, M. Prodanovic, C. Hernandez-Aramburu, and T. C. Green, "Energy Management in Autonomous Microgrid Using Stability-Constrained Droop Control of Inverters," *IEEE Transaction on Power Electronics*, vol. 23, pp. 2346-2351, 2008.